

Magnesium Fluoride (MgF_2)

THOMAS M. COTTER, MICHAEL C. THOMAS,
and WILLIAM J. TROPF

Applied Physics Laboratory
The Johns Hopkins University
Laurel, Maryland

Magnesium fluoride is a tetragonal material with TiO_2 (rutile) structure. The space group is D_{4h} or $P4_2/mnm$. The unit cell contains two fluorine units (six atoms). Dimensions of the cell (at 27 °C) are 0.4623 nm along the *a* axis and 0.3032 nm along the *c* axis [1, also see 2]. Theoretical density is 3.177 g/cm³ and melting point is 1528 ± 3 K [2]. A melting point of 1543 K is also reported [3].

Magnesium ions occupy octahedral sites with D_{3h} point symmetry. Six fluorine ions at sites with C_{3v} symmetry surround each magnesium ion. Fluorine-ion positions in the unit cell are known from X-ray diffraction measurements [1, 2].

A wide transparency range from 0.13 to 6 μm [2], good mechanical properties, and low optical index of refraction make magnesium fluoride a desirable material for coatings and interference filters. MgF_2 is a positive dispersive material, with its highest birefringence in the UV. Except for lithium fluoride, MgF_2 has the shortest wavelength cutoff of any common optical material.

Magnesium fluoride occurs naturally as the mineral sellaite [5]. Single-crystal MgF_2 [3, 4] is widely used for windows, lenses, polarizers, and other optical components. Optical-quality, hot-pressed polycrystalline MgF_2 is also used for optical components, particularly in the infrared. IRTRAN 1 [5] is a trade name for hot-pressed MgF_2 made by Kodak; KO-1 is an equivalent Soviet material [6]. Obara and McBratlie [7] compare properties of IRTRAN 1 and single-crystal magnesium fluoride.

MgF_2 has been used as a divalent-ion host material for solid-state lasers. Vanadium, nickel, and cobalt have been used as dopants to produce tunable solid-state lasers in the infrared [8, 9].

The UV and IR transparency of magnesium fluoride lends itself to many applications. MgF_2 has been used as a window material for UV detectors in space applications [10, 11]. The birefringence is used to polarize light in the UV [12-14]. One such polarizer, operating from the UV to the IR, has

been constructed [15]. The low index of MgF_2 in the IR (ed to its use as a Soleil compensator in the IR [16], Magnesium fluoride is also used as a thin film in coal aluminum nitrides for enhanced reflectivity in the vacuum UV [17, 18]. Because of the relatively low index, magnesium fluoride is also used as an antireflection coating for lenses and in a low-order layer in dielectric interference filters.

Magnesium fluoride has a band gap of approximately 11.8 eV. Optical constants from the UV through the XUV have been measured for single-crystal magnesium fluoride [19–22]. The lowest-energy electronic feature of the magnesium fluoride spectrum is an exciton peak centered near 11.8 eV [20, 21]. This is due to an exciton peak at 11.6 eV for the extraordinary component and at 12.2 eV for the ordinary component [22]. The exciton peak obscures the UV absorption edge in this region, measured at 10.9 eV [20]. Although an absorption band beginning at 1320 Å has been observed, the transmission does not drop significantly until 1190 Å (10.8 eV) [2], which is close to the measured absorption edge. The interband transitions begin near 12.2 eV [21], at 12.4 eV for the extraordinary and 12.6 eV for the ordinary ray [22]. The extraordianry-ray absorption curve has structure at 18.5 eV and the ordinary ray at 15 and 20.5 eV [22]. Broad absorption structure near 20.8 eV is attributed to interband transitions [20]. These transitions are believed to arise from transitions from the upper valence band of fluorine ($2p^6$) in the conduction band of magnesium ($3s+3p$) [21]. A peak at 24.5 eV is attributed to a plasmon [20, 22]. The plasmon peak is composed of an extraordinary-ray component at 24.3 eV and an ordinary-ray component at 24.6 eV [22]. Structure seen in the absorption coefficient from 22–40 eV is attributed to interband transitions from $2p^2$ level of the fluorine ion to the conduction band [19, 21]. In the 40–56 eV region, two absorption peaks exist: an absorption peak at 41.5 eV caused by a double plasmon and a peak at 54.6 eV attributed to an exciton [19]. Structure from 56–62 eV is attributed to transitions of $2p^4$ electrons of magnesium to the conduction band [19].

Refractive-index data for the MgF_2 transparent region from the UV through the IR are given by many sources [2, 12, 23–27]. Dodge [27] fitted index data (at 19°C) to a Sellmeier-type dispersion relationship of the form

$$\frac{n^2 - 1}{n^2 + 1} = \frac{2.9903553 \times 10^4}{(230,499.30)^2 - \nu^2} + \frac{4.4543708 \times 10^4}{(105,692.13)^2 - \nu^2} + \frac{4.0838897 \times 10^4}{(420,28101)^2 - \nu^2} \quad (1a)$$

and

$$\frac{n^2 - 1}{n^2 + 1} = \frac{3.0458729 \times 10^4}{(272,424.78)^2 - \nu^2} + \frac{6.1302694 \times 10^4}{(110,178.73)^2 - \nu^2} + \frac{4.4070663 \times 10^4}{(420,66305)^2 - \nu^2} \quad (1b)$$

where ν is the frequency in wave constant. Equation 1 represents electro-

one resonances with the first two terms and all IR resonances with the third term. These terms fall in the middle of the measured electrode transitions and lattice vibrations, respectively. The overall accuracy of index calculated from Eq. 1 is quoted as better than 3×10^{-4} over the 1400–30,000 cm^{-1} range.

Change in the index of refraction with temperature, pressure, and time is realistic. Thermo-optic data are given by many sources [2, 25–30] without good agreement; data from the National Bureau of Standards [26] are considered comprehensive, cover a wide temperature range, and agree well with recent measurements of the temperature dependence of optical dispersion [30]. The elastic properties of MgF_2 have been reported in the form of elastic constants, photoelastic constants, and piezoelectric constants [31, 32].

Optical properties of thin films of magnesium fluoride have been studied extensively. Much disparity exists between published data due to variations of the conditions and method of preparation of the sample under study [33–37]. In addition, thin-film properties usually do not match single-crystal properties [19, 20]. Consequently, this article concentrates on properties of single crystals.

Radiation damage of MgF_2 is described elsewhere [38]. Studies of extinction effects on the absorption of magnesium fluoride have revealed absorption bands in the UV. Three prominent absorption peaks at 317, 260, and 230 nm develop, which can be attributed to the formation of F^- centers by radiation [38]. No observations of IR absorption due to radiation have been reported [38]. The characterization of the fluorescence of MgF_2 has also been undertaken [39, 40].

Absorption at the IR edge of transparency is dominated by multiphonon absorption [40]. A model of multiphonon absorption [41] has been developed and confirmed with experimental data over a wide temperature range. Material constants for the ordinary ray of MgF_2 are given by Thomas and Joseph [42].

The fundamental (one-photon) lattice vibrations occur in the 290–625 cm^{-1} spectral region. Group theory predicts the following phonon modes for MgF_2 [43–46]:

$$\Gamma = A_{1g} + A_{1u} + A_{2u} + B_{1g} + B_{1u} + 2B_{2g} + E_g + 3E_u, \quad (2)$$

where the A_{2g} and B_{2g} modes are optically inactive, the A_{1g} ($E||c$) and E_g ($E \perp c$) modes are IR-active, and the remaining modes are Raman-active. Table I lists the IR modes as denoted by Barker [44], Thomas and Joseph [42], and Giudiceo and Banak [46]. Oscillations of the Raman modes are given by Porto et al. [45] as 92 (B_{1g}), 203 (E_g), 440 (A_{1g}), and 515 (B_{1u}) cm^{-1} .

Table I also lists both the transverse and longitudinal optical frequen-

ches. The transverse optical frequencies are the mode locations; the maximum longitudinal-mode frequency is an important parameter in the multiphonon-absorption model [41], since it designates the maximum phonon frequency.

At frequencies below the lowest-frequency transverse optical mode, absorption decreases and the material becomes transparent. The magnitude of absorption is thought to be a combination of contributions from both the tail of the fundamental lattice vibrations and various multiphonon difference bands. The index of refraction now also includes the effect of lattice vibrations. Estimates of low-frequency absorption made from the red wing of the fundamental modes (Table I) for MgF₂ are about 60% of the ordinary-ray imaginary index of refraction and 95% of the extraordinary-ray values, determined by Bystrov et al. [47] in the 10–35 cm⁻¹ region. Measurement of two different altered samples of polycrystalline MgF₂ by Stensil and Sisodia [48] showed yet higher absorption.

The low-frequency index of refraction of unagitated Euorite is given by Postanella et al. [49] at 1000 Hz and by Bystrov et al. [47] for the 300–200 GHz range. These data agree with each other and with the data in Table I (except for the slightly higher extraordinary-ray value given by Postanella et al. [49]). No temperature-dependent low-frequency index data were found, but pressure dependence is given by Ulrik et al. [30].

Table II was constructed from measurements reported in the literature as well as model predictions [51]. Real-index data (n) from 10–83 eV and Imaginary-Index (k) data from 11–83 eV are taken from several sources [19–22]. The measurements by Hansen et al. [19], Williams et al. [20], and Stephan et al. [31] did not distinguish between ordinary- and extraordinary-ray components. These data can be considered to be an "average" for the crystal. Thomas et al.'s [22] measurement of ordinary- and extraordinary-ray optical constants for the 11–29 eV region are also included.

Ordinary-ray index data in the 0.115–0.200 μm region are taken from Williams and Arslanov [23], supplemented by measurements of Steinonen et al. [12]. Extraordinary-ray data for this region are obtained by combining ordinary-ray data with the anomalous dispersion data of Chandrasekharan and Dauntary [24]. Both ordinary- and extraordinary-ray data in the 1400–50,000 cm⁻¹ range are calculated from the Sellmeier dispersion relationships (Eq. 1) of Dodge [27]. One value of ordinary-ray absorption coefficient is given by Andonova et al. [12].

Singit [51] and multiphonon [41] lattice-vibration models are used to estimate the complex index of refraction for wavelengths of 7.41 μm and longer. Measurements of Bystrov et al. [47], and Postanella et al. [49] are the best available low-frequency index data.

The accuracy of index measurements in the electronic region is relatively poor; estimated errors are approximately 10%. Data from Hansen et al.

[19] and Williams *et al.* [20] agree well in the overlap region (20–27 eV). Data from Stephan *et al.* [21] have consistently lower n and higher k compared with other sources [19, 20]. Data from Thomas *et al.* [22] have precision on the order of $\pm 5\%$.

The real-index data from 0.115–0.300 μm have a quoted accuracy of ± 0.002 ; the dispersion formula of Dodge [23] represents the data from 0.2–7.0 μm with ± 0.0002 . The accuracy of complex-index data at longer wavelength is unknown, but uncertainty in the values is probably in the least-significant digit reported in Table II (that is, n accurate to ± 0.01 and k to about 5%). Low-frequency real-index measurements of Paninevitch *et al.* [49] are given as accuracy of ± 0.003 . Bystrov *et al.* [47] quotes the accuracy of n to be ± 0.005 and k to be within $\pm 5\%$.

Figures 1 and 2 show a composite of the complex index of refraction based on the data of Table II. Figure 1 gives the ordinary-ray index and Fig. 2 shows the extraordinary-ray properties. Complex index-of-refraction data for the electronic region (wavelengths below 0.05 μm) derived from unpolarized measurements with an unknown mix of ordinary- and extraordinary-ray index are included in Fig. 1.

Tables III and IV give temperature dependences for the real part of the index of extinction. Measurements of dn/dT by Goldstein *et al.* [26] typically have a standard deviation to a linear temperature-dependence fit of $0.1 \times 10^{-4}/\text{K}$.

REFERENCES

1. G. M. O. Wheland, "Crystal Structures," Interscience Publishers, New York, 251 (1960).
2. A. Cernyukov and B. N. H. Stewarrov, "Some Properties of Magnesium Fluoride Crystallized from the Melt," *Proc. Phys. Soc. (London)* 73, 1001 (1958).
3. W. A. Ferguson, "Magnesium Fluoride Up-to-date Summary of Optical Properties," *Laser Focus* 18, 56 (1982).
4. "Crystal Optics," Chapter 69 in, Handbook of Crystal Science, CRC, 21 (1989).
5. "Kodak IRTRAN Selected Optical Materials," Publication U-12, Eastman Kodak Company, Rochester, New York, (1977).
6. I. V. Mele, R. K. Volynets, and Y. P. Savchenko, "The Spectroscopy of KCl-I Optic Ceramic," *Ves. J. Opt. Tech.* 25, 95 (1974).
7. A. L. Olson and W. B. McEvily, "Transmission of Single-Crystal Magnesium Fluoride and IRTRAN-I in the 0.2 to 15 μ Range," *J. Opt. Soc. Am.* 53, 1028 (1963).
8. L. P. Johnson and H. J. Guggenheim, "Porous-Thermated Optical Matrix," *Phys. Rev.* 170, 170 (1967).
9. P. F. Klemens, "Pulse-Potential Operation of Dithioc Transitive-Metal Lattice," *IEEE J. Quantum Electron.* QEP-18, 1137 (1982).
10. O. Grzegory, M. Gerasimow, B. Duszak, W. Rosler, and W. Mietnicki, "Fabrication of MgF_2 and LiF Windows for the Earth-Space Telescope Imaging Spectrograph," *Proc. SPIE* 3495, 136 (1998).
11. W. Witczak, A. G. Eustis, G. F. Parker, and J. E. Bagaysto, "Photoluminescent Window Materials under Electron Irradiation: Phosphorescence and Photoabsorption," *Appl. Opt.* 24, 2004 (1995).

12. D. L. Johnson, W. G. Phillips, M. Whicker, and F. F. Foster, "Polarizer for the Vacuum Ultraviolet," *Appl. Opt.*, **6**, 1009 (1967).
13. G. Hess and W. R. Hinzer, "Reflection Polarizers for the Vacuum Ultraviolet Using $\text{Al} + \text{MgF}_2$ Mixtures and an MgF_2 Plate," *Appl. Opt.*, **17**, 34 (1978).
14. W. C. Johnson, Jr., "Magnesium Fluoride Polarizing Plates for the Vacuum Ultraviolet," *Rev. Sci. Instrum.*, **25**, 1375 (1954).
15. G. C. Morris and A. S. Alphonso, "Single Surface Plates for Light Polarization Between 1400–70,000 Å," *Appl. Opt.*, **8**, 1349 (1969).
16. R. D. Park, "A MgF_2 Beam Compensator for the X-ray Infra-red," *Appl. Opt.*, **7**, 978 (1968).
17. W. R. Hinzer, J. P. Chomicki, and G. Hess, "Reflection of Aluminized Oxidized MgF_2 and CaF_2 in the Ultraviolet Region from 1500 Å to 360 Å at Various Angles of Incidence," *Appl. Opt.*, **11**, 240 (1972).
18. R. Jones and E. J. McCarthy, "Dyed Polyesters of Magnesium Oxidized Aluminized Glass in the UV (2000–2500 Å)," *Appl. Opt.*, **16**, 2316 (1977).
19. W. F. Phillips, E. T. Andrus, and M. W. Williams, "Optical Properties of MgO and MgF_2 in the Extreme Ultraviolet Region," *J. Appl. Phys.*, **43**, 4064 (1972).
20. M. W. Williams, R. A. McElroy, and R. T. Andrus, "Optical Properties of Magnesium Fluoride in the Vacuum Ultraviolet," *J. Appl. Phys.*, **38**, 1249 (1967).
21. O. Strobl, Y. Le Calvez, J. C. Letourneau, and B. Moret, "Properties Optiques et Spectre Electromagnétique de MgF_2 de 10 à 10-eV," *J. Phys. Chem. Solids*, **39**, 671 (1968).
22. J. Thomas, G. Stephen, J. C. Lecomte, M. Meyer, and S. Roche, "Optical Anisotropy of MgF_2 in the UV Ultraviolet Region," *Phys. Rev. Solid State*, **3**, 34, 163 (1952).
23. M. W. Williams and E. T. Andrus, "Optical Properties of Cylindrical MgF_2 from 115 to 400 nm," *Appl. Opt.*, **11**, 937 (1972).
24. V. Chaudhury and H. Duley, "Anisotropic Dispersion of Birefringence of Silicate and Magnesium Fluoride in the Vacuum Ultraviolet," *Appl. Opt.*, **6**, 671 (1967).
25. W. L. Wolfe, "Properties of Optical Anisotropy," in "Handbook of Optics" (W. L. Wolfe, ed.), McGraw-Hill, New York, 7–45 (1973).
26. H. H. Li, "Refractive Index of Alluvial Earth Flakes and its Wavelength and Temperature Derivatives," *J. Phys. Chem. Ref. Data*, **9**, 161 (1980).
27. M. J. Dodge, "Refractive Properties of Magnesium Fluoride," *Appl. Opt.*, **23**, 1969 (1984).
28. A. Polkova, D. Brownell, R. M. Whicker, and M. J. Dodge, "Optical Materials Characterization Final Technical Report, February 1, 1978–September 26, 1979," National Bureau of Standards Technical Note 973, 69 (February 1980).
29. F. G. Liedtke, A. K. Roy, L. W. Shuler, and J. A. Blau, "Thermal and Structural Considerations of Magnesium Fluoride and Zinc Sulfide for Optical Coating Applications," *Opt. Eng.*, **20**, 500 (1981).
30. D. P. Belanger, A. H. King, and V. Andronov, "Temperature Dependence of the Optical Birefringence of MgF_2 , MgF_3 , and BaF_2 ," *Phys. Rev. B*, **26**, 2626 (1982).
31. G. Dray, "Photoelastic Properties of Magnesium Fluoride," in "Basic Optical Properties of Materials. Summary of Papers," National Bureau of Standards Special Publication 524, 213 (1971).
32. I. I. Alphonso, L. E. Audubon, I. V. Mamonov, and V. M. Danilov, "Photoelastic Properties and Residual Stress in Magnesium Fluoride Crystals," *Russ. Phys. Solid State*, **17**, 2036 (1979).
33. D. Smith and P. Bernstein, "Refractive Index of Barium Oxide and Fluoride Casting Magnolia," *Appl. Opt.*, **18**, 111 (1979).
34. G. R. Wood III, M. G. Crispin, J. E. Schreyer, and Y. J. Makrory, "Vacuum Ultraviolet Loss in Magnesium Fluoride Films," *Appl. Opt.*, **13**, 3644 (1984).

35. P. J. Mants, W. G. Sabay, R. P. Neuberfield, G. R. McKenzie, G. J. G. Coetzeyen, S. F. St., G. R. Wood, and G. Q. Coignard, "Influence of Ion Assistance on the Optical Properties of MgF_2 ," *Appl. Opt.* **26**, 5235 (1987).
36. A. E. Barker and A. Lauzer, "Optical Transitions in Disordered Thin Films of the Ionic Compounds MgF_2 and AlF_3 as a Function of Their Conditions of Preparation," *Appl. Opt.* **16**, 2865 (1977).
37. J. M. Sánchez, R. Martínez, and L. E. Rodríguez, "Determinación de las Propiedades Ópticas del Oxígeno de MgF_2 y ZnF_2 a través de Medidas Espectrofotométricas en el Rango de Temperatura Media," *Appl. Opt.* **17**, 2549 (1988).
38. M. J. Walker, ed., "CRC Handbook of Appl. Science and Technology, Volume 3: Optical Materials, Part I: Non-Brittle Optical Properties/Radiation Damage," CRC Press, Boca Raton, FL, 334 (1989).
39. W. Vielkrause, A. G. Bobenko, G. P. Petry, and J. G. Borkelamp, "Photomultiplier Radiation Materials Under Electron Irradiation Fluorescence and Phosphorescence," *Appl. Opt.* **14**, 2194 (1975).
40. T. F. Gleiter, "Absorption Coefficients of Infrared Laser Windows Materials," *J. Phys. Chem. Solids* **34**, 3091 (1973).
41. M. E. Thomas, R. J. Joseph, and W. J. Tröpf, "Infrared Transmittance Properties of Sapphire, Spinel, Yttria, and ALON as a Function of Frequency and Temperature," *Appl. Opt.* **27**, 129 (1988).
42. M. E. Thomas and R. J. Joseph, "A Comparative Model for the Intrinsic Transmittance Properties of Optical Windows," *Proc. SPIE* **908**, 87 (1988).
43. G. R. Hunt and C. M. Peary, "Faraday Rotation and Dielectric Constants of Precision Magnesium Fluoride and Magnesium Fluoride," *Phys. Rev. Lett.* **A48** (1964).
44. A. S. Barker, "Transverse and Longitudinal Optic Mode Study in MgF_2 and ZnF_2 ," *Phys. Rev. B15*, A1190 (1974).
45. S. P. S. Porto, P. A. Maturi, and T. C. Dumon, "Raman Scattering of TiO_2 , MgF_2 , ZnF_2 , PbF_2 , and HgF_2 ," *Phys. Rev. B14*, 522 (1976).
46. J. Cirkvenac and C. Denević, "Infrared Spectra of Iron, Zinc, and Magnesium Fluorides: I. Analysis of Results," *J. Phys. C: Solid State Phys.* **11**, 2797 (1978).
47. V. P. Bykov, V. G. Oshchepkov, G. V. Kudin, and A. F. Kupriyanenko, "Dielectric Properties of Optical Crystals at Submillimeter Wavelengths," *Sov. Phys. Tech. Phys.* **31**, 1190 (1986).
48. M. Brana and G. Sánchez, "Near Infrared Wave Characterization of Dual Mode Multicells," *Appl. Opt.* **26**, 1279 (1988).
49. J. Pustovalov, C. Anderson, and D. Bonade, "Low-Frequency Dielectric Constants of α -Quartz, Sapphirine, MgF_2 , and MgO ," *J. Appl. Phys.* **48**, 2642 (1974).
50. J. Link, M. C. Kishoregulli, J. J. Pustovalov, V. B. Brava, and C. G. Anderson, "Dramatic Variation of the Low Frequency Dielectric Constant of Some Anisotropic Crystals," *J. Appl. Phys.* **45**, 396 (1981).
51. M. E. Thomas, "A Correlation Curve for Modeling Optical Properties of Window Materials," *Proc. SPIE* **1111**, 254 (1989).

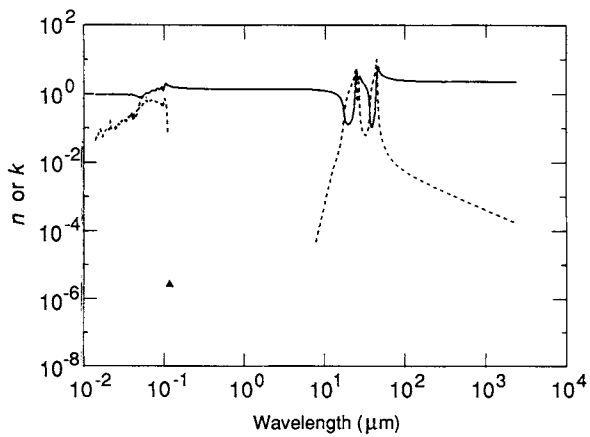


Fig. 1. Log-log plot of n_o (solid line) and k_o (dashed line) versus wavelength in micrometers for the ordinary ray of magnesium fluoride. Data below 0.05 μm (electronic region) are combined ordinary- and extraordinary-ray results.

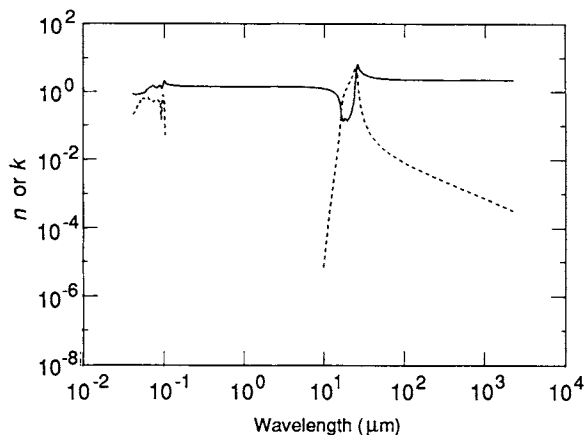


Fig. 2. Log-log plot of n_e (solid line) and k_e (dashed line) versus wavelength in micrometers for the extraordinary ray of magnesium fluoride.

TABLE I
Fundamental Infrared Lattice Vibration Parameters for MgF_2^a

Mode	Transverse optical frequency (cm ⁻¹)	Strength	Normalized width	Longitudinal optical frequency (cm ⁻¹)	Refs.
$E \perp c$ axis (ordinary ray)					
1	247	2.22	0.014	303	[44]
2	410	0.19	0.033	415	[44]
3	450	1.14	0.058	617	[44]
	Total = 3.55				
1	248	2.23	0.0115	302	[51]
2	408.5	0.22	0.0165	414	[51]
3	447	1.10	0.025	621	[51]
4 ^b	535	0.05	0.3		
	Total = 3.60				
1	251			304	[46]
2	413			422	[46]
3	452			610	[46]
	Total = 3.38				
$E \parallel c$ axis (extraordinary ray)					
1	399	2.7	0.048	625	[44]
2 ^c	556	0.01	0.08		
	Total = 2.71				
1	404	2.69		626	[46]

^aThe frequency (ν_j) is the location of the mode (transverse optical frequency). The strength ($\Delta\epsilon_j$) is the contribution of the mode to the dielectric constant. The normalized width (γ_j) is the mode width divided by the mode frequency. The complex dielectric constant (ϵ) is then modeled as a function of frequency (ν) by:

$$\epsilon(\nu) = \epsilon_{\infty} + \sum_j \frac{\Delta\epsilon_j \nu_j^2}{\nu_j^2 - \nu^2 + i\gamma_j \nu_j \nu},$$

where the ϵ_{∞} term (= 1.886 for $E \perp c$ and 1.918 for $E \parallel c$ axis) represents the electronic contributions to the dielectric constant (plus one).

^bMode 4 ($E \perp c$) is probably caused by an impurity.

^cBarker [44] identifies this as a weak forbidden mode.

TABLE II
Values of α and β Calculated from Various References for Migration Parameters

eV	α_{pp}^{-1}	α_{pp}	β_{pp}	k_{pp}	α_{pp}	β_{pp}	k_{pp}
50.0	669608	0.0149	0.906	[18]	0.046	[19]	
74.5	633411	0.0158	0.912		0.070		
76.5	620398	0.0161	0.905		0.064		
75.5	509314	0.0164	0.906		0.061		
74.5	508809	0.0167	0.902		0.063		
72.5	503604	0.0173	0.916		0.066		
54.5	571191	0.0161	0.902		0.049		
66.0	532322	0.0176	0.913		0.077		
53.0	504238	0.0151	0.917		0.076		
64.0	515151	0.0164	0.919		0.079		
53.0	504125	0.0157	0.921		0.063		
52.0	503060	0.0160	0.903		0.060		
57.0	441994	0.0163	0.924		0.065		
66.0	409629	0.0207	0.926		0.060		
55.0	423849	0.0190	0.926		0.059		
53.0	507198	0.0224	0.926		0.060		
57.0	439032	0.0176	0.923		0.062		
56.0	431667	0.0221	0.913		0.064		
55.0	442601	0.0199	0.926		0.063		
54.0	433155	0.0220	0.910		0.061		
53.0	427420	0.0294	0.926		0.068		
52.0	419403	0.0295	0.926		0.069		
51.0	417129	0.0293	0.923		0.100		
50.0	408274	0.0295	0.926		0.103		
49.0	399209	0.0285	0.922		0.107		
48.0	387143	0.0299	0.920		0.111		
47.5	383116	0.0284	0.920		0.113	0.067 [21]	0.062 [21]
47.0	399078	0.0284	0.929		0.113	0.066	0.066
46.5	375045	0.0267	0.929		0.118	0.055	0.059
46.0	371012	0.0270	0.919		0.123	0.054	0.053
45.5	366979	0.0274	0.926		0.122	0.053	0.053
45.0	362947	0.0276	0.929		0.121	0.049	0.050
44.5	338914	0.0279	0.928		0.121	0.046	0.114
44.0	334981	0.0282	0.929		0.121	0.047	0.115
43.5	330948	0.0285	0.918		0.124	0.046	0.113
43.0	349616	0.0269	0.926		0.122	0.036	0.109
42.5	342789	0.0285	0.928		0.123	0.034	0.110
42.0	338750	0.0285	0.918		0.125	0.033	0.109
41.5	334717	0.0285	0.918		0.124	0.044	0.129
41.0	330683	0.0285	0.919		0.124	0.047	0.131
40.5	326650	0.0286	0.921		0.127	0.050	0.139
40.0	322617	0.0210	0.919		0.123	0.059	0.149
39.5	318585	0.0214	0.919		0.157	0.056	0.158
39.0	314554	0.0218	0.920		0.174	0.054	0.159

(continued)

TABLE II (Continued)

Magnesium Fluoride

eV	cm ⁻¹	μm	π	δ	n	k
38.5	310521	0.0322	0.922	0.173	0.298	0.170
38.0	306486	0.0326	0.927	0.173	0.292	0.168
37.5	302456	0.0331	0.923	0.174	0.291	0.169
37.0	298423	0.0337	0.924	0.175	0.290	0.168
36.5	294390	0.0340	0.922	0.175	0.289	0.168
36.0	290357	0.0344	0.927	0.175	0.288	0.169
35.5	286324	0.0348	0.924	0.175	0.287	0.168
35.0	282293	0.0354	0.923	0.175	0.286	0.167
34.5	278269	0.0358	0.922	0.177	0.285	0.168
34.0	274236	0.0363	0.904	0.179	0.283	0.176
33.5	270204	0.0370	0.299	0.162	0.280	0.188
33.0	266171	0.0376	0.298	0.169	0.282	0.206
32.5	262138	0.0381	0.291	0.200	0.287	0.204
32.0	258105	0.0387	0.287	0.240	0.280	0.221
31.5	254073	0.0394	0.204	0.219	0.287	0.199
31.0	250040	0.0403	0.310	0.228	0.288	0.269
30.5	246007	0.0407	0.310	0.232	0.287	0.233
30.0	241974	0.0413	0.307	0.228	0.283	0.233
29.5	237942	0.0420	0.298	0.224	0.286	0.233
29.0	233909	0.0426	0.287	0.221	0.283	0.187
28.5	229866	0.0426	0.273	0.234	0.280	0.164
28.0	225833	0.0433	0.287	0.254	0.282	0.269
27.5	221801	0.0431	0.153	0.261	0.271	0.223
27.0	217768	0.0439	0.162	0.272	0.222	0.227
26.5	213735	0.0446	0.124	0.382	0.132	0.246
26.0	209702	0.0477	0.301	0.398	0.398	0.367
25.5	205670	0.0485	0.767	0.358	0.787	0.294
25.0	201637	0.0494	0.779	0.361	0.771	0.234
24.5	197604	0.0505	0.767	0.443	0.738	0.361
24.0	193572	0.0517	0.767	0.326	0.735	0.410
23.5	189539	0.0529	0.416	0.610	0.742	0.442
23.0	185506	0.0539	0.156	0.581	0.266	0.473
22.5	181473	0.0551	0.107	0.721	0.630	0.386
22.0	177441	0.0564	0.985	0.771	0.949	0.564
21.5	173408	0.0577	1.012	0.852	0.899	0.534
21.0	169375	0.0590	1.101	0.919	0.994	0.614
20.5	165342	0.0603	1.134	0.956	0.983	0.643
20.0	161309	0.0610	1.268	0.787	0.981	0.946
19.5	157277	0.0610			0.953	0.943
19.5	153244	0.0633			1.009	0.545
19.4	156470	0.0639			0.994	0.445
19.3	154437	0.0676			1.001	0.603
19.0	153244	0.0653			1.012	0.615
18.4	139631	0.0639			1.021	0.648

(continued)

TABLE II (Continued)
Magnetic Fluctuations

eV	cm^{-1}	μm	a	b	c	d
16.3	150010	0.0657			1.094	0.636
16.4	149496	0.0674			1.044	0.626
16.2	146792	0.0684			1.073	0.661
16.0	145179	0.0699	1.322 [30]	0.697 [30]	1.093	0.661
17.8	143566	0.0657	1.387	0.699	1.083	0.624
17.6	141352	0.0704	1.342	0.677	1.193	0.661
17.4	140598	0.0713	1.085	0.690	1.144	0.660
17.2	138726	0.0724	1.329	0.687	1.086	0.665
17.0	137113	0.0739	1.084	0.685	1.080	0.668
16.8	135300	0.0750	1.348	0.685	1.188	0.670
16.6	133687	0.0747	1.346	0.681	1.145	0.676
16.4	132274	0.0756	1.348	0.686	1.180	0.679
16.2	130860	0.0765	1.387	0.573	1.146	0.684
16.0	130458	0.0773	1.404	0.540	1.193	0.679
15.9	129041	0.0780	1.448	0.538	1.195	0.680
15.8	127435	0.0789	1.487	0.531	1.199	0.625
15.7	126028	0.0790	1.463	0.538	1.193	0.620
15.6	125420	0.0799	1.424	0.528	1.171	0.626
15.5	125013	0.0800	1.431	0.538	1.190	0.617
15.4	124208	0.0804	1.480	0.531	1.196	0.628
15.3	123400	0.0810	1.481	0.533	1.209	0.651
15.2	122593	0.0816	1.380	0.538	1.238	0.615
15.1	121388	0.0821	1.345	0.548	1.289	0.638
15.0	120880	0.0822	1.358	0.531	1.255	0.630
14.9	120176	0.0832	1.510	0.530	1.257	0.633
14.8	119369	0.0838	1.512	0.510	1.257	0.644
14.7	118563	0.0843	1.513	0.501	1.257	0.655
14.6	117756	0.0849	1.509	0.501	1.238	0.660
14.5	116949	0.0855	1.484	0.502	1.267	0.650
14.4	116143	0.0861	1.485	0.504	1.268	0.646
14.3	115336	0.0862	1.451	0.514	1.269	0.593
14.2	114530	0.0873	1.470	0.518	1.268	0.578
14.1	113723	0.0879	1.473	0.517	1.239	0.627
14.0	112917	0.0885	1.485	0.501	1.237	0.697
13.9	112110	0.0892	1.524	0.494	1.234	0.617
13.8	111304	0.0895	1.541	0.485	1.231	0.608
13.7	110497	0.0905	1.561	0.477	1.235	0.593
13.6	109691	0.0912	1.573	0.463	1.238	0.605
13.5	108884	0.0918	1.584	0.453	1.242	0.608
13.4	108077	0.0923	1.588	0.444	1.235	0.605
13.3	107271	0.0922	1.585	0.438	1.224	0.594
13.2	106464	0.0928	1.583	0.433	1.315	0.595
13.1	105658	0.0946	1.585	0.436	1.286	0.573
13.0	104851	0.0934	1.581	0.430	1.192	0.568

(continued)

TABLE II (Continued)
Magnesium Fluoride

eV	cm ⁻¹	μm	π_0	k_0	π_r	k_r
12.9	104045	0.0984	1.366	0.389	1.192	0.363
12.8	103236	0.0969	1.379	0.387	1.186	0.360
12.7	102432	0.0956	1.374	0.382	1.177	0.358
12.6	101628	0.0944	1.361	0.381	1.172	0.358
12.5	100824	0.0932	1.409	0.364	1.138	0.355
12.4	100012	0.1603	1.336	0.408	1.232	0.346
12.3	99205	0.1606	1.269	0.451	1.242	0.378
12.2	98399	0.1616	1.291	0.481	1.184	0.377
12.1	97592	0.1623	1.207	0.502	1.177	0.355
12.0	96786	0.1603	1.351	0.472	1.176	0.370
11.9	95979	0.1642	1.304	0.563	1.231	0.329
11.8	95173	0.1651	1.293	0.573	1.343	0.354
11.7	94367	0.1662	1.372	1.024	1.477	0.381
11.6	93560	0.1669	1.201	0.807	1.373	0.322
11.5	92753	0.1679	2.306	0.463	1.647	0.356
11.4	91946	0.1688	2.284	0.424	1.613	0.373
11.3	91139	0.1697	2.239	0.372	1.589	0.340
11.2	90333	0.1703	2.123	0.226	1.427	0.476
11.1	89527	0.1717	2.210	0.110	1.590	0.341
11.0	88720	0.1723	1.584	0.039	1.519	0.162
10.9	87914	0.1737	1.306		1.460	0.026
10.8	87107	0.1743	1.343		1.460	
10.7	86301	0.1759	1.812		1.469	
10.6	85494	0.1770	1.233		1.463	
10.5	84687	0.1781	1.734		1.469	
10.4	83881	0.1792	1.354		1.466	
10.3	83074	0.1804	1.646		1.463	
10.2	82267	0.1816	1.660		1.469	
10.1	81461	0.1828	1.443		1.466	
10.0	80655	0.1840	1.591		1.463	
eV	cm ⁻¹	μm	π_0	k_0	π_r	k_r
27.0	217966	0.0439	0.611 [24]	0.214 [22]	0.611 [22]	0.214 [24]
26.5	214375	0.0448	0.795	0.240	0.616	0.233
26.0	210783	0.0457	0.784	0.241	0.608	0.241
25.5	207190	0.0465	0.770	0.303	0.730	0.361
25.0	203607	0.0466	0.765	0.361	0.794	0.385
24.5	197988	0.0505	0.776	0.598	0.799	0.332
24.0	194372	0.0517	0.363	0.402	0.807	0.367
23.5	190759	0.0528	0.734	0.611	0.816	0.408
23.0	187146	0.0539	0.790	0.436	0.827	0.441
22.5	183533	0.0551	0.805	0.488	0.877	0.448
22.0	179921	0.0564	0.897	0.489	0.867	0.396

(continued)

TABLE II (Continued)

Simpler Than 2

νN	$\omega \text{ s}^{-1}$	$\omega \text{ rad}$	R_s	A_s	R_e	A_e
21.5	173408	0.0577	0.395	0.545	0.366	0.596
21.0	169975	0.0590	0.398	0.500	0.361	0.614
20.5	165342	0.0593	1.005	0.501	0.394	0.612
20.0	161310	0.0600	1.010	0.610	0.300	0.607
19.5	157277	0.0616	1.005	0.541	0.319	0.607
19.0	153344	0.0633	1.000	0.560	0.363	0.525
18.5	149311	0.0670	1.004	0.572	1.117	0.632
18.0	145179	0.0683	1.000	0.604	1.151	0.632
17.5	141146	0.0705	1.000	0.591	1.364	0.525
17.0	137113	0.0726	1.000	0.632	1.317	0.575
16.5	133080	0.0751	1.000	0.595	1.333	0.564
16.0	129048	0.0773	1.000	0.607	1.415	0.396
15.5	125015	0.0810	1.000	0.581	1.313	0.496
15.0	120983	0.0827	1.004	0.596	1.367	0.305
14.5	116949	0.0855	1.003	0.568	1.269	0.390
14.0	112917	0.0880	1.007	0.525	1.272	0.320
13.5	108885	0.0893	1.043	0.514	1.346	0.339
13.0	104853	0.0954	1.046	0.407	1.449	0.306
12.5	100821	0.0945	1.061	0.385	1.353	0.469
12.0	96788	0.0984	1.102	0.406	1.419	0.496
11.5	92756	0.1000	1.023	0.549	1.479	0.324
11.0	88723	0.1030	1.062	0.308	1.346	0.151
10.5	84690	0.1050	1.099	0.274	1.223	0.463
10.0	80657	0.1051	1.013	0.630	1.343	0.223
9.5	76625	0.1049	1.043	0.515	1.296	0.777
9.0	72593	0.1066	1.014	0.380	1.311	0.615
8.5	68560	0.1107	1.000	0.341	1.366	0.400
8.0	64528	0.1137	1.036	0.069	1.361	0.054
7.5	60504	0.1137			1.362	
7.0	56471	0.1146			1.274	
6.5	52439	0.115	1.714 [39]		1.007 ^a	
6.0	48406	0.1159			1.057 [22]	
5.5	44373	0.120	1.626		1.026 ^b	
5.0	40340	0.1212		1.3-10 ⁻⁴ [22]		
4.5	36308	0.123	1.368		1.597 ^c	
4.0	32275	0.130	1.453		1.567 ^c	
3.5	28243	0.140	1.513		1.527 ^c	
3.0	24210	0.150	1.494		1.497 ^c	
2.5	20178	0.140	1.465		1.478 ^c	
2.0	16145	0.170	1.451		1.468 ^c	
1.5	12113	0.1780	1.3995 [12]		1.43363 [12]	
1.0	8088	0.140	1.346	[22]		
0.5	50555	0.1650	1.3424 [22]		1.44397	
0.0	50533	0.199	1.339	[22]		

(continued)

TABLE II (Continued)
Magnesium Fluoride

ν	cm^{-1}	μm	λ_{ν}	λ_{α}	λ_{ν}	λ_{α}
6.199	74060	0.308	1.42427 [27]		1.42437 [27]	
5.994	747610	0.210	1.41754		1.41763	
5.686	45455	0.220	1.42291		1.42298	
5.391	43478	0.220	1.40900		1.40904	
5.166	41667	0.240	1.40547		1.40550	
4.959	40000	0.230	1.40280		1.40282	
4.766	73462	0.230	1.40130		1.40130	
4.597	39037	0.220	1.39912		1.39917	
4.429	35714	0.220	1.39620		1.39627	
4.273	34483	0.230	1.39430		1.39430	
4.133	35353	0.230	1.39288		1.39294	
4.009	32258	0.210	1.39163		1.39162	
3.873	31290	0.330	1.39040		1.39075	
3.757	30343	0.330	1.38934		1.39160	
3.647	39412	0.340	1.38830		1.39030	
3.542	25571	0.330	1.38732		1.38964	
3.444	27779	0.330	1.38634		1.38875	
3.351	27027	0.370	1.38560		1.38790	
3.263	24216	0.360	1.38510		1.38723	
3.179	23641	0.360	1.38448		1.38658	
3.100	24020	0.400	1.38387		1.39394	
2.952	23810	0.400	1.38381		1.39462	
2.818	27727	0.400	1.38378		1.39389	
2.695	21759	0.400	1.38180		1.38936	
2.593	20803	0.400	1.38040		1.39223	
2.480	30020	0.430	1.38078		1.39164	
2.394	19031	0.330	1.37923		1.39111	
2.295	18519	0.340	1.30873		1.39039	
2.214	17887	0.360	1.37829		1.39013	
2.138	17241	0.500	1.37769		1.38871	
2.066	16667	0.400	1.37792		1.38903	
2.000	16129	0.400	1.37718		1.38887	
1.937	14623	0.400	1.37629		1.38805	
1.879	15152	0.400	1.37629		1.38933	
1.823	14706	0.400	1.37633		1.38908	
1.771	14896	0.300	1.37668		1.38932	
1.722	13889	0.120	1.37363		1.38736	
1.673	13514	0.200	1.37303		1.38735	
1.621	13158	0.180	1.37344		1.38714	
1.590	12823	0.200	1.37324		1.38893	
1.560	12500	0.200	1.37206		1.38874	
1.533	12195	0.200	1.37448		1.38835	
1.498	11905	0.200	1.37472		1.38839	
1.442	11628	0.200	1.37446		1.38822	

(continued)

TABLE II (Continued)
Magnetic Fluorescence

ν	cm^{-1}	μm	R_p	k_p	R_s	k_s
1.009	11364	0.960	1.37440		1.38606	
1.078	11111	0.960	1.37426		1.38596	
1.346	10870	0.960	1.37411		1.38573	
1.119	12639	0.960	1.37506		1.38603	
1.202	10447	0.960	1.37384		1.38546	
1.365	12204	0.960	1.37371		1.38533	
1.240	10009	1.000	1.37352		1.38510	
1.215	9800	1.000	1.37344		1.38506	
1.190	9600	1.0417	1.37335		1.38492	
1.165	9400	1.0634	1.37318		1.38479	
1.141	9208	1.0870	1.37306		1.38464	
1.116	9000	1.1111	1.37290		1.38449	
1.208	9800	1.1364	1.37277		1.38434	
1.366	9800	1.1620	1.37268		1.38418	
1.243	9400	1.1904	1.37247		1.38402	
1.017	6300	1.3193	1.37221		1.38385	
0.5819	9000	1.2904	1.37213		1.38307	
0.4601	7800	1.2631	1.37197		1.38348	
0.9423	7000	1.3126	1.37179		1.38329	
0.9175	7800	1.3514	1.37160		1.38309	
0.8927	7200	1.3469	1.37140		1.38287	
0.8679	7000	1.3088	1.37118		1.38265	
0.8431	6800	1.4704	1.37096		1.38240	
0.8183	6800	1.3132	1.37071		1.38214	
0.7935	6400	1.3634	1.37046		1.38193	
0.7687	6200	1.0128	1.37017		1.38156	
0.7439	6800	1.5657	1.36985		1.38136	
0.7191	5800	1.2341	1.36959		1.38096	
0.6943	5400	1.7837	1.36937		1.38049	
0.6695	7400	1.3019	1.36913		1.38007	
0.6447	5200	1.3031	1.36883		1.37965	
0.6199	5000	2.8040	1.36854		1.37907	
0.6675	4800	2.0409	1.36827		1.37879	
0.6427	4800	2.0635	1.36820		1.37849	
0.5927	4700	2.1227	1.36809		1.37817	
0.5579	4600	2.1739	1.36803		1.37787	
0.6379	4800	2.2222	1.36873		1.37747	
0.5421	4400	2.2727	1.36877		1.37706	
0.5531	4400	2.8220	1.36859		1.37667	
0.7307	4207	2.3610	1.36818		1.37623	
0.5683	4109	2.4590	1.36879		1.37576	
0.4921	4000	2.6000	1.36928		1.37525	
0.4623	3800	2.4641	1.36973		1.37471	
0.4711	3800	2.6518	1.36929		1.37410	

(continued)

TABLE II (Continued)
Magnesium Fluoride

eV	cm^{-1}	μm	n_g	k_g	n_b	k_b
0.4587	3700	2.7087	1.36261		1.37348	
0.4663	3600	2.7716	1.36196		1.37279	
0.4339	3700	2.8871	1.36106		1.37184	
0.4211	3400	2.9412	1.36049		1.37122	
0.4977	3500	3.0303	1.35986		1.37038	
0.3968	3700	3.1250	1.35874		1.36934	
0.3884	3100	3.2258	1.35773		1.36827	
0.3720	3000	3.3353	1.35663		1.36707	
0.3750	2900	3.2683	1.35739		1.36579	
0.3472	3800	3.5714	1.35402		1.36429	
0.3348	3700	3.7087	1.35249		1.36246	
0.3294	3800	3.8463	1.35107		1.36100	
0.3160	2900	4.0690	1.36003		1.35173	
0.2974	3400	4.1567	1.36003		1.34837	
0.2852	2900	4.3678	1.34442		1.35166	
0.2728	2900	4.5483	1.34120		1.35040	
0.2604	2106	4.7619	1.33792		1.34704	
0.3880	3000	5.2086	1.33404	$4.2 \cdot 10^{-2}$ [31]	1.36388	
0.2418	1900	5.1282	1.35246	$4.0 \cdot 10^{-2}$	1.34034	
0.2458	1900	5.2482	1.35246	$8.5 \cdot 10^{-3}$	1.34799	
0.2294	1900	5.4054	1.35089	$1.2 \cdot 10^{-1}$	1.31521	
0.2237	1900	5.5356	1.35088	$1.7 \cdot 10^{-1}$	1.33217	
0.2171	1730	5.7143	1.35085	$2.5 \cdot 10^{-1}$	1.32989	
0.2108	1700	5.8824	1.31754	$3.6 \cdot 10^{-1}$	1.31578	
0.2046	1650	6.0694	1.31370	$5.1 \cdot 10^{-1}$	1.32114	
0.1984	1600	6.2240	1.30961	$7.4 \cdot 10^{-1}$	1.31666	
0.1922	1550	6.4318	1.30487	$1.1 \cdot 10^{-1}$	1.31134	
0.1860	1600	6.6567	1.29978	$1.4 \cdot 10^{-1}$	1.30611	
0.1798	1450	6.8968	1.26584	$2.4 \cdot 10^{-1}$	1.29946	
0.1734	1400	7.1498	1.24740	$3.7 \cdot 10^{-1}$	1.29260	
0.1676	1390	7.4074	1.261 [31]	$5.7 \cdot 10^{-1}$	1.288 [31]	
0.1613	1300	7.8624	1.229	$9.4 \cdot 10^{-1}$	1.277	
0.1550	1240	8.0000	1.264	$1.3 \cdot 10^{-1}$	1.269	
0.1488	1300	8.3339	1.332	$1.8 \cdot 10^{-1}$	1.257	
0.1426	1130	8.6857	1.240	$2.3 \cdot 10^{-1}$	1.248	
0.1364	1100	9.0396	1.284	$3.4 \cdot 10^{-1}$	1.237	
0.1302	1060	9.3238	1.366	$7.1 \cdot 10^{-1}$	1.206	
0.1240	1000	10.0000	1.19	$1.3 \cdot 10^{-1}$	1.18	
0.1175	980	10.204	1.17	$1.5 \cdot 10^{-1}$	1.17	
0.1100	960	10.417	1.16	$1.9 \cdot 10^{-1}$	1.16	
0.1138	960	10.586	1.15	$2.4 \cdot 10^{-1}$	1.15	
0.1143	920	10.870	1.14	$3.8 \cdot 10^{-1}$	1.13	
0.1146	900	11.111	1.12	$3.7 \cdot 10^{-1}$	1.12	
0.1099	240	11.384	1.11	$4.4 \cdot 10^{-1}$	1.10	

(continued)

TABLE II (Continued)
Wavelength Wavelengths

eV	cm^{-1}	nm	R_s	k_s	R_v	k_v
0.0001	350	11.628	1.09	$5.7 \cdot 10^{-3}$	1.09	
0.0003	340	11.608	1.07	$6.9 \cdot 10^{-3}$	1.06	
0.0017	330	11.191	1.06	$8.4 \cdot 10^{-3}$	1.06	
0.0002	330	12.300	1.03	0.008	1.01	
0.0007	320	12.323	0.98	0.012	0.99	
0.0042	310	13.198	0.93	0.015	0.94	
0.0017	310	13.514	0.91	0.018	0.91	
0.0030	310	13.809	0.91	0.022	0.94	$7.3 \cdot 10^{-3}$ [31]
0.0009	300	14.206	0.79	0.028	0.78	0.011
0.0040	290	14.706	0.71	0.040	0.69	0.021
0.0018	290	15.162	0.61	0.053	0.59	0.029
0.0094	280	15.623	0.47	0.11	0.48	0.084
0.0069	270	16.128	0.38	0.14	0.38	0.26
0.0044	270	16.367	0.17	0.30	0.14	0.38
0.0010	270	17.241	0.14	0.72	0.14	0.78
0.0064	260	17.457	0.14	0.96	0.16	0.99
0.0050	260	18.319	0.14	1.4	0.15	1.1
0.0043	260	19.281	0.13	1.5	0.14	1.4
0.0030	260	20.000	0.17	1.9	0.15	1.7
0.0050	250	20.408	0.21	2.2	0.17	1.4
0.0053	250	20.823	0.37	2.5	0.19	2.1
0.0053	250	21.377	0.47	3.1	0.23	2.1
0.0070	250	21.729	0.96	4.9	0.27	2.1
0.0078	250	22.322	3.11	5.3	0.36	2.1
0.0046	240	22.787	4.97	1.4	0.46	2.1
0.0073	240	23.296	3.56	0.98	0.38	3.7
0.0033	240	23.818	2.99	0.91	1.06	4.4
0.0068	240	24.390	2.79	2.2	2.19	3.5
0.0066	240	25.000	3.36	0.99	1.09	3.3
0.0064	230	25.561	2.74	0.17	6.97	5.3
0.0071	230	26.316	2.49	0.12	5.15	1.1
0.0096	230	27.027	3.21	0.094	4.45	0.68
0.0045	220	27.778	2.92	0.072	2.98	0.49
0.0034	220	28.371	1.96	0.290	3.61	0.28
0.0030	220	29.412	1.96	0.068	2.41	0.21
0.0069	210	29.303	1.46	0.071	3.22	0.14
0.0097	210	31.250	1.39	0.083	3.03	0.15
0.0034	210	32.386	0.81	0.13	5.93	0.11
0.0037	200	35.333	0.18	0.64	2.48	0.000
0.0066	200	34.483	0.11	1.4	2.78	0.074
0.0047	200	37.714	0.11	2.0	2.09	0.063
0.0034	200	37.887	0.13	2.8	3.87	0.037
0.0023	200	38.462	0.32	4.4	2.91	0.000
0.0010	200	40.000	3.25	9.9	7.12	0.000

(continued)

TABLE II (Continued)
Magnesium Fluoride

ν	cm^{-1}	μP	τ_{ν}	k_{ν}	τ_k	k_k
0.0296	240	41.667	6.19	0.49	2.48	0.089
0.0295	230	43.678	4.43	0.14	2.44	0.084
0.0273	230	45.455	3.70	0.072	2.41	0.081
0.0260	210	47.617	3.40	0.042	2.38	0.077
0.0248	230	50.000	3.15	0.072	2.35	0.073
0.0236	190	52.622	2.99	0.032	2.33	0.070
0.0223	180	55.536	2.87	0.019	2.31	0.069
0.0211	170	58.624	3.70	0.015	2.29	0.068
0.0198	180	62.500	2.30	0.013	2.27	0.066
0.0186	150	66.467	2.04	0.011	2.25	0.065
0.0174	140	71.426	2.39	$9.3 \cdot 10^{-3}$	2.24	0.063
0.0161	130	76.403	2.34	$8.0 \cdot 10^{-3}$	2.22	0.062
0.0149	120	81.373	2.31	$7.0 \cdot 10^{-3}$	2.21	0.061
0.0138	110	90.904	2.48	$6.1 \cdot 10^{-3}$	2.20	$5.1 \cdot 10^{-3}$
0.0124	100	101.00	2.45	$5.2 \cdot 10^{-3}$	2.19	$4.3 \cdot 10^{-3}$
0.0113	90	111.11	2.43	$4.5 \cdot 10^{-3}$	2.18	$3.5 \cdot 10^{-3}$
0.0099	80	125.00	2.40	$3.9 \cdot 10^{-3}$	2.16	$3.3 \cdot 10^{-3}$
0.0087	70	142.86	2.39	$3.3 \cdot 10^{-3}$	2.17	$3.0 \cdot 10^{-3}$
0.0079	60	165.57	2.38	$2.8 \cdot 10^{-3}$	2.17	$2.7 \cdot 10^{-3}$
0.0063	50	200.00	2.37	$2.3 \cdot 10^{-3}$	2.16	$2.3 \cdot 10^{-3}$
0.0059	40	250.00	2.38	$1.8 \cdot 10^{-3}$	2.16	$2.1 \cdot 10^{-3}$
0.0057	30	333.33	2.19	$1.3 \cdot 10^{-3}$	2.15	$2.1 \cdot 10^{-3}$
0.0029	23.3	428.57	2.259 [47]	$1.4 \cdot 10^{-1}$ [47]	2.190 [47]	$2.8 \cdot 10^{-3}$ [47]
0.0023	20	500.0	2.25 [51]	$5.7 \cdot 10^{-1}$ [51]	2.15 [51]	$1.5 \cdot 10^{-3}$ [51]
0.0021	16.7	600.0	2.245 [47]	$1.4 \cdot 10^{-1}$ [47]	2.181 [47]	$1.7 \cdot 10^{-3}$ [47]
0.0019	15	666.67	2.26 [51]	$5.5 \cdot 10^{-1}$ [51]	2.15 [51]	$1.1 \cdot 10^{-3}$ [51]
0.0012	10	1000.0	2.235 [47]	$1.0 \cdot 10^{-1}$ [47]	2.173 [47]	$8.0 \cdot 10^{-4}$ [47]
			2.26 [51]	$4.3 \cdot 10^{-1}$ [51]	2.15 [51]	$7.0 \cdot 10^{-4}$ [51]
0.0006	5	2000.0	2.24	$2.1 \cdot 10^{-1}$	2.15	$2.8 \cdot 10^{-4}$
0.0000	-0	—	2.24	0	2.15	0
			2.243 [49]		2.197 [49]	

*Reference site indicated in brackets.

^aOrdinary data from Wildegis and Andrade [23] and anomalous dispersion data from Chandrasekharan and Damay [24] are combined to estimate extraband-ray index.

TABLE III

Values of dn_o/dT Obtained from Various References for Magnesium Fluoride

eV	cm^{-1}	μm	dn_o/dT (1/K)	Notes
2.708	21839	0.4579	$1.47 \cdot 10^{-6}$	20°C [28]
1.959	15803	0.6328	$1.12 \cdot 10^{-6}$	20°C [28]
1.078	8696	1.15	$0.88 \cdot 10^{-6}$	20°C [28]
0.366	2950	3.39	$1.1 \cdot 10^{-6}$	20°C [28]
0.0	≈ 0	—	$1.0 \cdot 10^{-4}$	Our data [51]

TABLE IV

Values of dn_e/dT Obtained from Various References for Magnesium Fluoride

eV	cm^{-1}	μm	dn_e/dT (1/K)	Notes
2.708	21839	0.4579	$0.86 \cdot 10^{-6}$	20°C [28]
1.959	15803	0.6328	$0.58 \cdot 10^{-6}$	20°C [28]
1.078	8696	1.15	$0.32 \cdot 10^{-6}$	20°C [28]
0.366	2950	3.39	$0.6 \cdot 10^{-6}$	20°C [28]